Macromolecules

Article

pubs.acs.org/Macromolecules

Synthesis and Characterization of New Selenophene-Based Donor–Acceptor Low-Bandgap Polymers for Organic Photovoltaic Cells

Woo-Hyung Lee,[†] Seon Kyoung Son,[‡] Kyoungkon Kim,[‡] Sang Kyu Lee,[§] Won Suk Shin,[§] Sang-Jin Moon,[§] and In-Nam Kang*[,†]

[†]Department of Chemistry, The Catholic University of Korea, Bucheon, Korea

[‡]Solar Cell Research Center, Korea Institute of Science and Technology, Seoul, Korea

[§]Energy Materials Research Division, Korea Research Institute of Chemical Technology, Daejeon, Korea

Supporting Information

ABSTRACT: A series of novel thiophene- and selenophene-based low-bandgap polymers were synthesized using a Stille cross-coupling reaction; these polymers contained quinoxaline and diketopyrrolopyrrole as acceptors. Various acceptors were introduced into the selenophene backbones, and the solubility, absorption spectra, energy levels, charge transport, blend film morphology, and photovoltaic properties of the resulting polymers were investigated. The weight-averaged molecular weights (M_w) of P3TDTQ, P3SDTQ, P3TDTDPP, and P3SDTDPP were found to be 12 300, 15 500, 13 300, and 17 200, with polydispersity indices of 1.46, 1.85, 1.58, and 1.63, respectively. Photophysical studies revealed low bandgaps of 1.70 eV for P3TDTQ, 1.63 eV for P3SDTQ, 1.27 eV for P3TDTDPP, and 1.25 eV for P3SDTDPP; the films could harvest a broad solar spectrum, covering the range from 300 to 800 nm (P3TDTQ and P3SDTQ) and from 350 to 950 nm (P3TDTDPP and P3SDTDPP). Solution-processed field-effect transistors fabricated from these polymers had p-type organic thin film transistor characteristics. The field-effect mobilities of P3TDTQ, P3SDTQ, P3TDTDPP, and P3SDTDPP were measured to be 2.8×10^{-5}, 5.0×10^{-5}, 1.0×10^{-3}, and 2.1×10^{-3} cm^2 V^{-1} s^{-1}, respectively. The novel polymers were combined with a PCBM ([6,6]-phenyl C_{71}-butyric acid methyl ester) acceptor to fabricate bulk heterojunction solar cells, which produced power conversion efficiencies of 0.64–3.18% under AM 1.5 G (100 mW/cm^2) conditions.

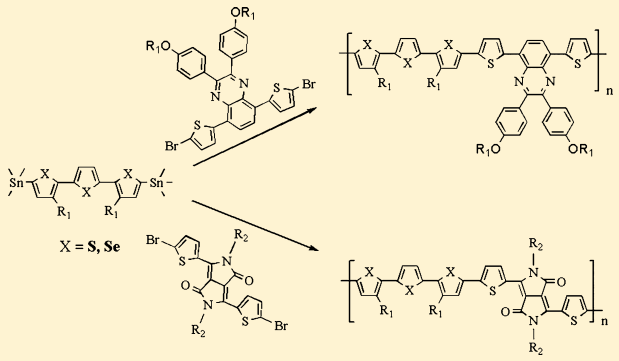

INTRODUCTION

Organic solar cells based on conjugated polymers have the potential to be applied as a clean energy source. In addition, such cells have the advantages that they can be fabricated at low cost via solution-based processing and that they have mechanical flexibility appropriate for foldable or rollable substrates.[1−4] Bulk-heterojunction (BHJ) devices—in which a donor polymer (p-type) is blended with a fullerene derivative or other acceptor (n-type) material—have emerged as the most efficient polymer solar cells (PSCs) developed to date.[5−7] One of the main factors limiting the performance of PSCs is the mismatch between their absorption and the terrestrial solar spectra. Polymer materials with low bandgaps are therefore needed to harvest solar photons at longer wavelengths, particularly in the near-IR region, and with a broader spectrum. Conjugated polymers that incorporate alternating donor and acceptor units produce significant decreases in the bandgap, due to the introduction of intramolecular charge transfer (ICT) structures.[8−10] Several types of donor–acceptor (D–A) conjugated copolymers have been synthesized for use in high-performance organic photovoltaic (OPV) applications. The use of thiophene as a donating moiety and quinoxaline (Qx) and diketopyrrolopyrrole (DPP) as accepting moieties has been closely investigated and provides a successful strategy to achieve low-bandgap materials.[11,12] Compared with their thiophene analogues, selenophene-containing polymers have been studied to a lesser extent, possibly due to the difficulties associated with their synthesis. As a class, polyselenophenes are expected to have advantages over polythiophenes. For example, interchain charge transfer should be facilitated by the intermolecular Se–Se contact, which means that polyselenophenes should have higher bulk conductivities and mobilities than polythiophenes.[13] Furthermore, selenophene substitution in conjugated polymers reduces the bandgap energy, mainly by stabilizing the lowest unoccupied molecular orbital (LUMO) level more effectively than the corresponding polythiophenes.[14−16] Poly(3-hexylselenophene) (P3HS) displays a bandgap energy (1.6 eV) lower than that of P3HT (1.9 eV).[15] The photovoltaic

Received: September 2, 2011
Revised: December 12, 2011
Published: January 31, 2012

   dx.doi.org/10.1021/ma2020112 | *Macromolecules* 2012, 45, 1303–1312

Scheme 1. Synthetic Routes for the Monomers

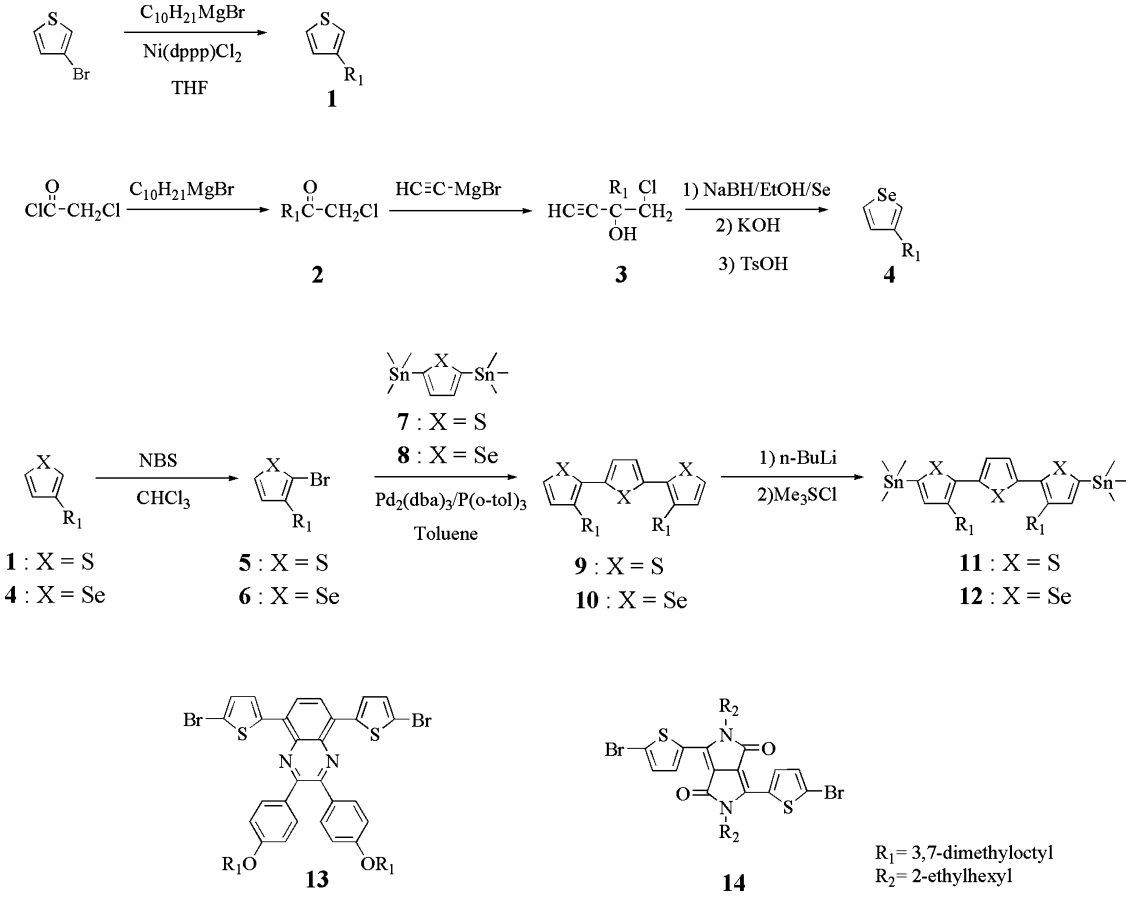

Scheme 2. Synthesis of the Low-Bandgap Polymers P3TDTQ, P3SDTQ, P3TDTDPP, and P3SDTDPP

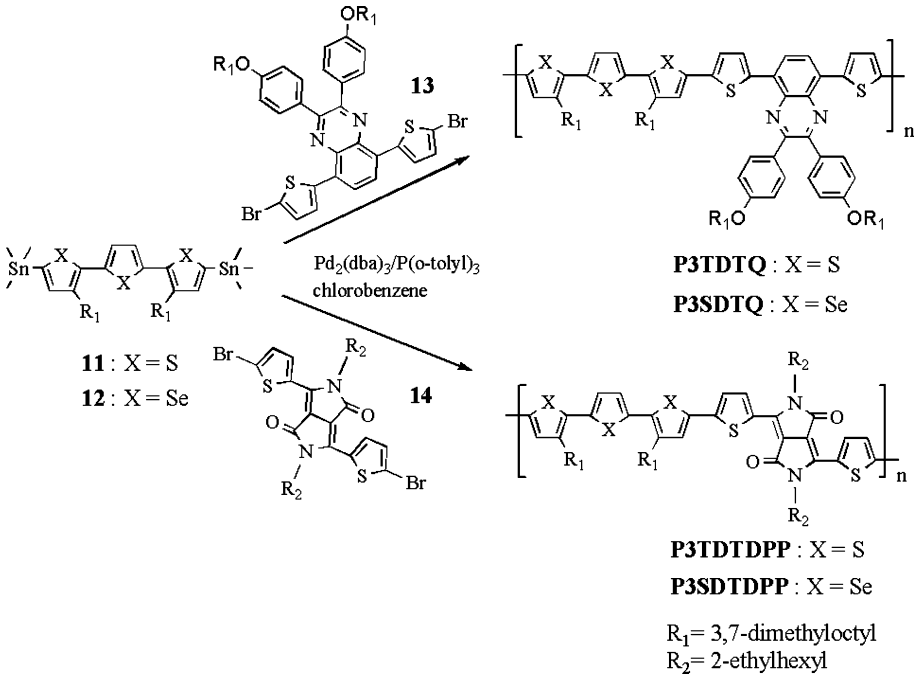

properties of P3HS:PCBM devices result in a high power conversion efficiency (2.7%) because P3HS provides a more extensive photon absorption cross section than P3HT.[14] Poly(3,3-dialkylterselenophene) (PSSS) also exhibits high charge-carrier mobilities and ambipolar behaviors in organic field effect transistor devices; the low LUMO energy levels are thought to facilitate both electron injection and transport.[16] Recently, several groups have reported the use of selenophene-

dx.doi.org/10.1021/ma2020112 | Macromolecules 2012, 45, 1303−1312

based D−A copolymers (with a selenophene donor and various acceptors) for organic transistors, but the solar cell performances of these polymers have not yet been reported.[17,18] Here, we report the synthesis, optical and physical properties, and OPV performances of novel selenophene-based D−A low-bandgap polymers. These polymers were synthesized using a Stille cross-coupling reaction, with terselenophene as a donor and quinoxaline (Qx) and diketopyrrolopyrrole (DPP) as acceptors. The Qx-containing polymers are denoted as P3SDTQ, and those containing DPP are denoted as P3SDTDPP. These polymers have lower bandgaps in π-conjugated polymers, thereby increasing the overall photon absorption by extending the spectral sensitivity. We examined the effects of the incorporation of different acceptors in the selenophene backbones on the absorption, energy levels, charge transport properties, morphologies, and photovoltaic properties of the donor/acceptor blends. In addition, terthiophene-based D−A polymers (with terthiophene as a donor and quinoxaline (Qx) (P3TDTQ) and diketopyrrolopyrrole (DPP) (P3TDTDPP) as acceptors) were also synthesized using the same polymerization method, to allow a comparison between the optoelectronic and photovoltaic properties of the terthiophene-based D−A polymers and those of the selenophene-based polymers.

RESULTS AND DISCUSSION

Synthesis and Characterization. The synthetic routes to the monomers and polymers are shown in Schemes 1 and 2, respectively. As shown in Scheme 1, a branched alkyl chain was introduced at the 3-position of the thiophene and selenophene rings to increase the solubility of the D−A copolymers. Compounds **1** and **4** were converted into the dibromo compounds **5** and **6** with *N*-bromosuccinimide (NBS) in the presence of a polar protic solvent, with good yields. Compounds **7** and **8** were synthesized according to methods described in the literature.[19,20] Compounds **9** and **10** were synthesized using the Stille coupling reaction, via the condensation of the distannyl compounds **7** and **8** and the corresponding brominated compounds **5** and **6**. Compounds **11** and **12** were synthesized from compounds **9** and **10** by distannylation, with good yields (68−91%). The P3TDTQ, P3SDTQ, P3TDTDPP, and P3SDTDPP polymers were obtained via the combinatorial Stille coupling reaction of compounds **11** and **12** with compounds **13** and **14**. The synthetic routes used to synthesize the P3TDTQ, P3SDTQ, P3TDTDPP, and P3SDTDPP polymers are also described in Scheme 2. The weight-average molecular weights (M_w) of P3TDTQ, P3SDTQ, P3TDTDPP, and P3SDTDPP were determined using gel permeation chromatography (GPC), using a polystyrene standard in a chloroform eluent; they were found to be 12 300 (PDI = 1.46), 15 500 (PDI = 1.85), 13 300 (PDI = 1.58), and 17 200 (PDI = 1.63), respectively. The polymer readily dissolved in common organic solvents such as toluene, chloroform, and THF and formed good films. Thermal analysis of the polymers was conducted using differential scanning calorimetry (DSC), and thermogravimetric analysis (TGA), as shown in Figure 1. The results showed that both polymers had good thermal stability over 300 °C, and no obvious thermal transitions were observed between 50 and 200 °C. The polymerization results for the synthesized copolymers are summarized in Table 1.

Optical and Electrochemical Properties. The UV−vis absorption spectra of the copolymers are shown in Figure 2 for

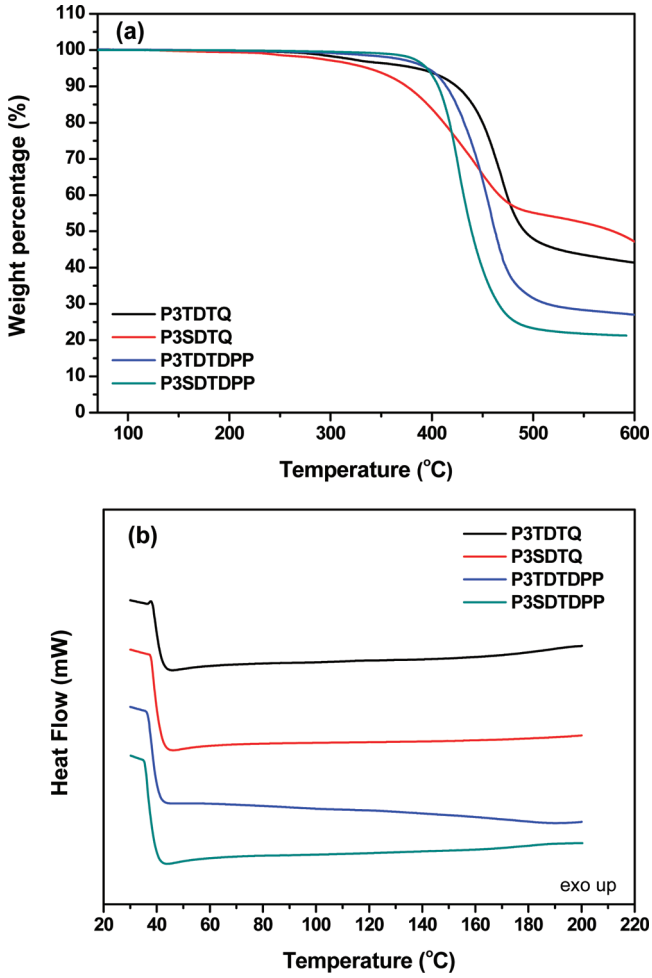

Figure 1. (a) TGA and (b) DSC of P3TDTQ, P3SDTQ, P3TDTDPP, and P3SDTDPP, performed at a heating rate of 10 °C min^{-1} under an inert atmosphere.

Table 1. Physical Properties of the Synthesized Polymers

polymer	M_n (g/mol)	M_w (g/mol)	PDI	T_d (°C)[a]
P3TDTQ	8.39K	12.3K	1.46	384
P3SDTQ	9.31K	15.5K	1.85	336
P3TDTDPP	8.43K	13.3K	1.58	395
P3SDTDPP	10.5K	17.2K	1.63	394

[a]Decomposition temperature at 5% weight loss.

copolymers in a dilute chlorobenzene solution and in thin films; the absorption data for the polymers are summarized in Table 2. The λ_{max} of P3TDTQ, P3SDTQ, P3TDTDPP, and P3SDTDPP in solution occurred at 549, 599, 679, and 702 nm, respectively, whereas those in the thin films occurred at 587, 619, 716, and 753 nm, respectively; these values were significantly red-shifted compared with those of poly(3,3-dialkylterthiophene) (PTT, $\lambda_{max,film}$ = 510 nm) and poly(3,3-dialkylterselenophene) (PSSS, $\lambda_{max,film}$ = 614 nm).[16,21] The UV−vis absorption spectra of the P3S-based polymers (P3SDTQ and P3SDTDPP) were red-shifted by about 20−50 nm with respect to those of the P3T-based polymers (P3TDTQ and P3TDTDPP), both in solution and in thin films; this resulted from the presence of selenium atoms in the polymer repeat units. Selenium atoms are more electron-rich than sulfur atoms; hence, aromatic rings containing selenium

dx.doi.org/10.1021/ma2020112 | Macromolecules 2012, 45, 1303−1312

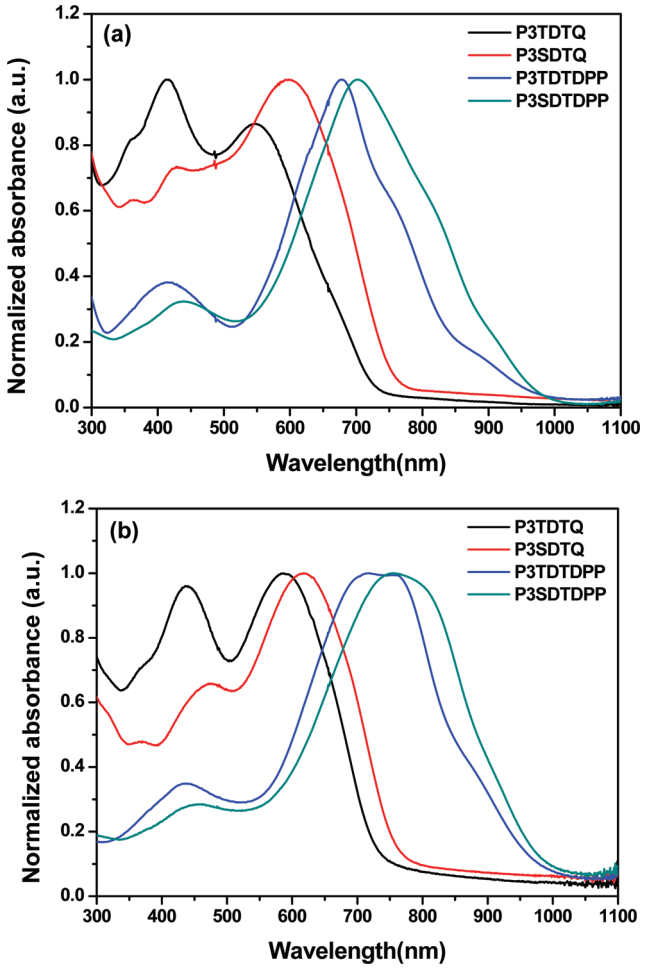

Figure 2. UV−vis spectra of P3TDTQ, P3SDTQ, P3TDTDPP, and P3SDTDPP (a) in chlorobenzene solution and (b) in thin films.

Table 2. UV−vis Maximum Absorption Wavelength (λ_{max}), Bandgap Energy (E_g), and Ionization Potential (E_{HOMO}) of P3TDTQ, P3SDTQ, P3TDTDPP and P3SDTDPP[a]

polymer	solution (λ_{max}, nm)[a]	film (λ_{max}, nm)	E_g^{opt} (eV)[b]	E_{HOMO} (eV)[c]	E_{LUMO} (eV)
P3TDTQ	431, 549	436, 587	1.70	−5.37	−3.67
P3SDTQ	428, 599	427, 619	1.63	−5.35	−3.72
P3TDTDPP	679	716	1.27	−5.21	−3.94
P3SDTDPP	702	753	1.25	−5.16	−3.91

[a]Measurements performed in chlorobenzene. [b]Estimated from the onset of the absorption in thin films (E_g = 1240/λ_{onset} eV). [c]Calculated using the optical bandgap energy.

are more easily delocalized than those containing sulfur atoms.[15,22,23] Moreover, the absorption spectra of the DPP-containing polymers (P3TDTDPP and P3SDTDPP) were red-shifted by over 130 nm compared with the spectra of the Qx-containing polymers (P3TDTQ and P3SDTQ), suggesting the presence of stronger $\pi-\pi$ interchain associations and aggregation in the solid state. Such aggregation is beneficial for improving charge mobility in thin films. The optical bandgaps of the polymer thin films were determined from the UV−vis absorption onsets in the solid state (E_g = 1240/λ_{onset} eV). The optical bandgaps (E_g) in the thin films were 1.70, 1.63, 1.27, and 1.25 eV for P3TDTQ, P3SDTQ, P3TDTDPP, and P3SDTDPP, respectively; these values were significantly lower than those found for poly(3,3-dialkylterthiophene) (PTT, 2.1 eV) and poly(3,3-dialkylterselenophene) (PSSS, 1.8 eV). This successful reduction in the bandgap was mainly due to intramolecular charge transfer (ICT) effects between the terthiophene donor or terselenophene donors and the Qx or DPP acceptor groups. The DPP moiety was a stronger acceptor than Qx, which led to a smaller E_g for P3TDTDPP and P3SDTDPP than for P3TDTQ and P3SDTQ. The low bandgaps of P3TDTDPP (1.27 eV) and P3SDTDPP (1.25 eV) may have resulted from the planarity and high degree of conjugation in the DPP acceptor, which would enhance the $\pi-\pi$ interactions and ICT among the polymer main chains.[24−26] Moreover, the optical bandgaps of the P3S-based polymer thin films were smaller than those of the P3T-based polymers because of the electron-rich selenium atoms in the core repeat units. The significant broadening in the absorption spectra of P3TDTDPP and P3SDTDPP (relative to P3TDTQ and P3SDTQ) may have indicated better ordering of the molecules in the bulk phase, which was manifested in the behavior of the external quantum efficiency (EQE).

Cyclic voltammograms (CV) are shown in Figure 3 for the polymers. These measurements were performed in an electro-

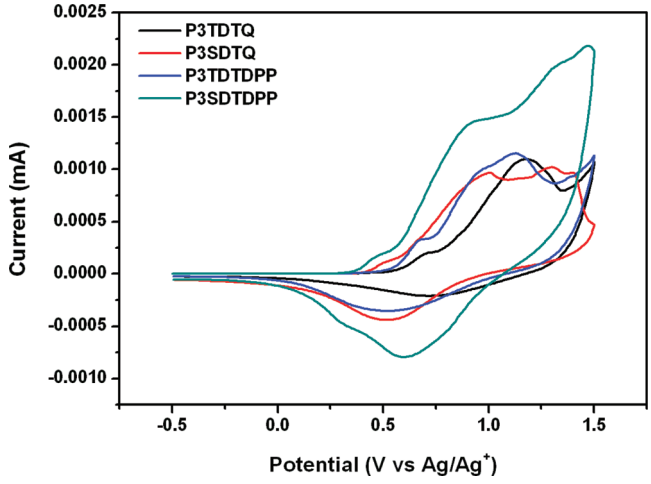

Figure 3. Cyclic voltammograms for the polymer films on ITO glass, performed at a scanning rate of 50 mV s^{-1}, in acetonitrile containing 0.1 M n-Bu_4NBF_4.

lyte solution of 0.1 M tetrabutylammonium tetrafluoroborate ($TBABF_4$) in anhydrous acetonitrile, at room temperature and under nitrogen, with a scan rate of 50 mV/s. The HOMO levels of the polymer films were estimated from the cyclic voltammograms, using the equation $E_{HOMO} = -(E_{ox} + 4.8)$ eV, where E_{ox} is the onset oxidation potential relative to the ferrocene standard material.[27] The highest occupied molecular orbital (HOMO) energy levels of P3TDTQ, P3SDTQ, P3TDTDPP, and P3SDTDPP were calculated to be −5.37, −5.35, −5.21, and −5.16 eV, respectively, using the ferrocene reference value of −4.8 eV below the vacuum level. The LUMO levels of P3TDTQ, P3SDTQ, P3TDTDPP, and P3SDTDPP were calculated to be −3.67, −3.72, −3.94, and −3.91 eV, respectively, as estimated from the optical bandgaps and HOMO energy levels. The deep HOMO levels may have contributed to the improved oxidative stability and higher open-circuit voltage (V_{oc}) compared with those of PTT (−5.2 eV) and PSSS (−4.9 eV).[16] The above results indicated that the bandgap and molecular energy levels of P3T- or P3S-based

dx.doi.org/10.1021/ma2020112 | Macromolecules 2012, 45, 1303−1312

polymers could be efficiently tuned by incorporating appropriate electron-withdrawing Qx and DPP groups. The electrochemical potentials are summarized in Table 2.

Field-Effect Transistor Characteristics. The effects of the shape and position of the side chains on the electrical transport properties of the resulting polymers were examined by measuring the field-effect transistor (FET) mobility. The field-effect carrier mobilities of the polymers were investigated by fabricating thin-film transistors with a bottom-contact geometry, using Au electrodes. The FET characteristics were determined under ambient conditions, and no precautions were taken to insulate the materials and devices from exposure to air, moisture, or light. The field-effect mobility was calculated according to the equation[28]

saturated regime ($V_D > V_G$):

$$I_D = (W/2L)\mu C_i(V_G - V_T)^2$$

where I_D is the drain current in the saturated regime, W and L are the channel width and length, respectively, μ is the field-effect mobility, C_i is the capacitance per unit area of the gate dielectric layer, and V_G and V_T are the gate and threshold voltages, respectively. The P3TDTQ, P3SDTQ, P3TDTDPP, and P3SDTDPP samples exhibited typical p-type organic semiconductor characteristics, with hole mobilities of 2.8×10^{-5}, 5.0×10^{-5}, 1.0×10^{-3}, and 2.1×10^{-3} $cm^2\ V^{-1}\ s^{-1}$, respectively. The results are plotted in Figure S1 (Supporting Information). The hole mobility values for the P3S-based polymers were ~1.5 times higher than those for the P3T-based polymers. The hole mobilities of the DPP-containing polymers (P3TDTDPP and P3SDTDPP) were 2 orders of magnitude higher than those of the Qx-containing polymers (P3TDTQ and P3SDTQ). The higher mobilities measured for P3TDTDPP and P3SDTDPP can be understood in terms of an improved intermolecular $\pi-\pi$ stacking, which corresponds well with the UV–vis results. In addition, P3TDTDPP and P3SDTDPP yielded higher hole mobilities than P3TDTQ and P3SDTQ; this was attributed to the more efficient charge extraction in the P3TDTDPP and P3SDTDPP solar cell devices (Table 3).

Table 3. PSC Performances of the Polymer/$PC_{61}BM$ Device

polymer	ratio	J_{SC} (mA/cm^2)	V_{OC} (V)	FF (%)	PCE (%)
P3TDTQ	1:1	1.29	0.68	34	0.30
	1:3	1.82	0.67	46	0.56
P3SDTQ	1:1	2.12	0.67	35	0.52
	1:3	2.48	0.63	45	0.72
P3TDTDPP	1:1	6.50	0.56	51	1.88
	1:3	5.25	0.56	51	1.49
P3SDTDPP	1:1	9.18	0.50	40	1.85
	1:3	6.45	0.51	41	1.36

Organic Photovoltaic Characteristics. Polymer solar cell devices were fabricated using the P3T- and P3S-based polymers as electron donors and [6,6]-phenyl C_{61}-butyric acid methyl ester ($PC_{61}BM$) as an electron acceptor. The device structure was ITO/PEDOT:PSS(50 nm)/polymer:$PC_{61}BM$/LiF(0.6 nm)/Al(130 nm). The photovoltaic performances of the polymer:$PC_{61}BM$ devices are summarized in Table 3 and Figure 4. The PCEs varied considerably with the polymer:PCBM blend ratio used in the devices; the details of the variation depended on the polymer backbone. Thus, the PCE

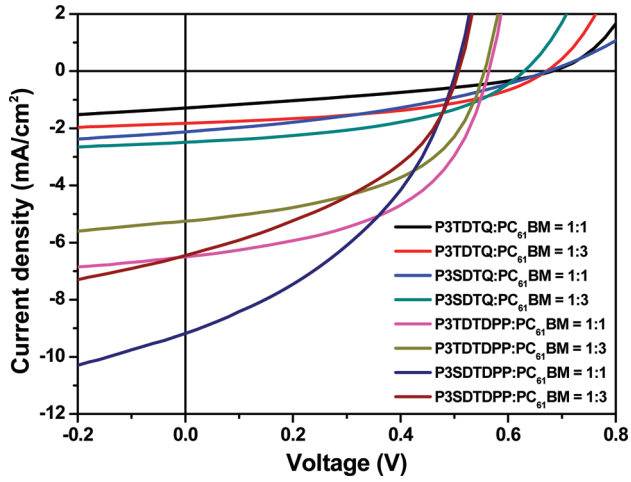

Figure 4. $J-V$ characteristics of a photovoltaic device using polymer/$PC_{61}BM$ blend films as active layers.

of the Qx-containing polymer devices was higher for a blend ratio of 1:3 than 1:1, while for DPP-containing polymer devices, the PCE was better with a 1:1 blend ratio than with a ratio of 1:3. The PCEs of the P3TDTQ, P3SDTQ, P3TDTDPP, and P3SDTDPP devices were found to be 0.30%, 0.52%, 1.88%, and 1.85%, respectively. The open-circuit voltages (V_{OC}, which is related to the difference between the HOMO level of the donor polymer and the LUMO level of the acceptor ($PC_{61}BM$)) of the P3TDTQ, P3SDTQ, P3TDTDPP, and P3SDTDPP devices were found to be 0.68, 0.67, 0.56, and 0.50 V, respectively, for a blend ratio of 1:1. The high V_{OC} values for the P3TDTQ and P3SDTQ devices could be explained by the low HOMO energy levels of P3TDTQ (−5.37 eV) and P3SDTQ (−5.35 eV) compared with those of P3TDTDPP (−5.21 eV) and P3SDTDPP (−5.16 eV). Among the devices using the P3T- and P3S-based polymers, the P3TDTDPP and P3SDTDPP devices demonstrated better photovoltaic performances than did those using P3TDTQ and P3SDTQ because the photon absorption fraction and the FET mobility were higher in the DPP-containing polymer films than in those containing Qx. The DPP-containing polymer devices therefore exhibited a high short circuit current density (J_{SC}). In the case of the Qx-containing polymer devices, the P3S-Qx devices showed higher PCE values than their thiophene analogues; however, the PCEs of the P3S-DPP devices were slightly lower than those of the P3T-DPP devices. The PCEs of the P3T-and P3S-based devices were heavily dependent on the electron-withdrawing accepting units. Interestingly, regardless of the PCE values of the devices, the P3S-based devices (Qx and DPP) always showed higher J_{SC} values than the corresponding thiophene analogues (for the same PCBM blend ratio). The increased short circuit currents of the P3S-based devices could be attributed to the increased spectral breadth of the absorbed photons and hole mobilities. To better understand the origin of the differences in the photovoltaic performances of the polymer solar cells, AFM images of the surface morphologies of each solar cell device were collected (Figure S2, Supporting Information). Generally, nanoscale phase separation should be established to allow efficient charge separation; this is true due to the short exciton diffusion length (~10 μm) of the donor polymers.[29] As can be seen in Figure S2, the P3TDTDPP:PCBM (1:1) and P3SDTDPP:PCBM (1:1) films showed a smoother and more interconnected network

dx.doi.org/10.1021/ma2020112 | Macromolecules 2012, 45, 1303–1312

of polymer−PCBM domains, which accounted for the high photocurrent density in these films. In contrast, relatively high levels of aggregation were observed in the P3TDTQ:PCBM (1:1) and P3SDTQ:PCBM (1:1) films, which reduced the area for charge separation, leading to a low photocurrent. There were no significant differences between the morphologies of the P3T-based films and those of the P3S-based films.

The performances of the solar cells based on P3TDTDPP:PCBM (1:1) and P3SDTDPP:PCBM (1:1) films were further enhanced via the use of [6,6]-phenyl C_{71}-butyric acid methyl ester ($PC_{71}BM$) as an electron acceptor and the use of a mixed chlorobenzene (CB)/1,8-diiodoctane (DIO) (97%:3% by volume) solvent. Figure 5 shows the current−

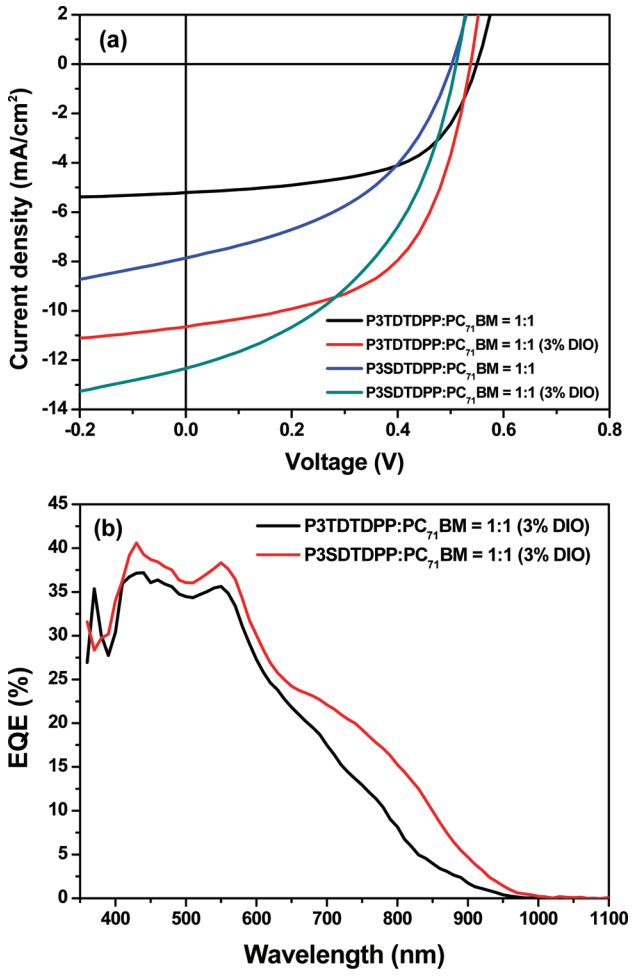

Figure 5. (a) $J-V$ characteristics of a photovoltaic device using P3TDTDPP/$PC_{71}BM$ (1:1) and P3SDTDPP/$PC_{71}BM$ (1:1) and (b) external quantum efficiency of the P3TDTDPP/$PC_{71}BM$ (1:1) and P3SDTDPP/$PC_{71}BM$ (1:1) blend films prepared from mixed CB/DIO (97/3, v/v) solvents.

voltage characteristics resulting from the use of the $PC_{71}BM$ and the mixed solvent in the polymer solar cell devices; the data are summarized in Table 4. The P3TDTDPP:$PC_{71}BM$ (1:1) and P3SDTDPP:$PC_{71}BM$ (1:1) devices showed PCE values similar to those shown by the corresponding $PC_{61}BM$ devices. In contrast, dramatic improvements were observed in the J_{SC} and PCE values for the 3% DIO-containing devices. The PCE increased from 1.88% to 3.18% for the P3TDTDPP:$PC_{71}BM$ (1:1) device and from 1.85% to 2.81% for the

Table 4. PSC Performances of the Polymer/$PC_{71}BM$ Device

polymer	ratio	J_{SC} (mA/cm^2)	V_{OC} (V)	FF (%)	PCE (%)
P3TDTDPP	1:1	5.21	0.55	58	1.65
	1:1[a]	10.65	0.54	56	3.18
P3SDTDPP	1:1	7.86	0.50	45	1.77
	1:1[a]	12.33	0.51	45	2.81

[a]3% DIO additive (v/v).

P3SDTDPP:$PC_{71}BM$ (1:1) device. In this case, the PCE of the P3SDTDPP device was slightly lower than that of the P3TDTDPP device, due to the low V_{OC} and FF; however, the J_{SC} of the P3SDTDPP device was higher than that of the P3TDTDPP device, which was attributed to the lower bandgap and higher mobility of the P3SDTDPP film (compared with the P3TDTDPP film). The improvement in the OPV performances was caused by the changes in the morphology of the blend film. AFM images (Figure. 6) clearly showed that there were large domains in the blend film prepared using only chlorobenzene; these large domains would diminish exciton migration to the donor/acceptor interface and are not favorable for charge separation. The morphology of the blend film prepared using the chlorobenzene/DIO mixed solvent was much more uniform, with no significant phase separation. Good miscibility between the donor polymer and the $PC_{71}BM$ was shown, and interpenetrating networks were formed; these factors may have led to increases in the J_{SC} value.

EQE values (which were measured to evaluate the photoresponses of the fabricated solar cells as a function of wavelength) are shown in Figure 5b for the P3TDTDPP:$PC_{71}BM$ (1:1) and P3SDTDPP:$PC_{71}BM$ (1:1) devices prepared with 3% DIO. The P3TDTDPP and P3SDTDPP devices yielded an EQE plot that was similar to the absorption spectra of P3TDTDPP and P3SDTDPP in the long wavelength region, indicating that excitons were mainly generated in the polymer phase. The spectral responses of the P3TDTDPP device showed that in the region from 350 to 950 nm photons contributed significantly to the EQE, with a maximum EQE of 35% at 550 nm. The P3SDTDPP device, however, exhibited an even better spectral response in the range 350−1000 nm, with a maximum EQE of 38% at 550 nm. The P3SDTDPP:$PC_{71}BM$ blend film exhibited a wide absorption spectrum (650−1000 nm), which resulted in a much higher J_{SC} of 12.33 mA/cm^2.

CONCLUSIONS

In summary, we successfully synthesized novel thiophene- and selenophene-based low-bandgap polymers, using the Stille coupling reaction. The P3TDTQ P3SDTQ, P3TDTDPP, and P3SDTDPP polymers showed good solubility in common organic solvents because of the presence of alkyl side chains. P3TDTQ, P3SDTQ, P3TDTDPP, and P3SDTDPP exhibited long-wavelength UV−vis absorption peaks at 587, 619, 716, and 753 nm, respectively. The P3SDTDPP:$PC_{71}BM$ blend film showed a wide absorption spectrum (650−1000 nm), which resulted in a much higher J_{SC} of 12.33 mA/cm^2. A photovoltaic device using the P3TDTDPP:$PC_{71}BM$ (1:1) and P3SDTDPP:$PC_{71}BM$ (1:1) films with added DIO as the active layer exhibited open-circuit voltages of 0.54 and 0.51 V, short-circuit current densities of 10.65 and 12.33 mA/cm^2, fill factors of 0.56 and 0.45, and power conversion efficiencies of 3.18 and 2.81% for the two films, respectively, under AM 1.5G (100 mW/cm^2) illumination. We believe that the V_{OC} and FF values

dx.doi.org/10.1021/ma2020112 | Macromolecules 2012, 45, 1303−1312

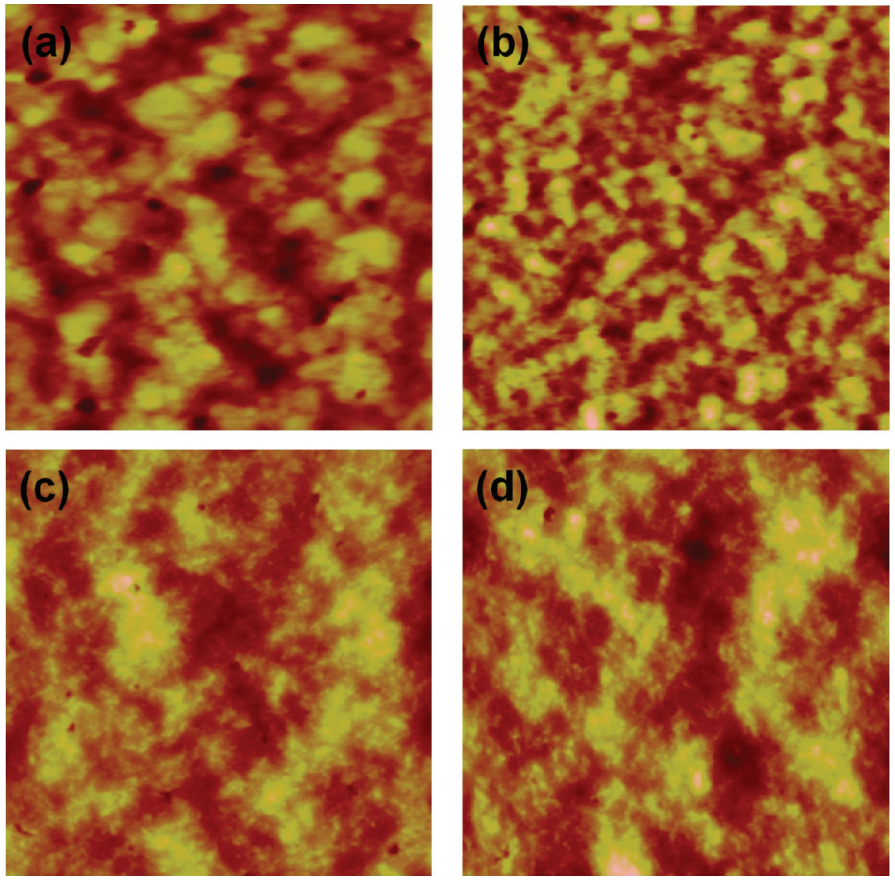

Figure 6. AFM tapping-mode height images of (a) P3TDTDPP/$PC_{71}BM$ (1:1), (b) P3SDTDPP/$PC_{71}BM$ (1:1), (c) P3TDTDPP/$PC_{71}BM$ (1:1) + 3% DIO, and (d) P3SDTDPP/$PC_{71}BM$ (1:1) + 3% DIO. The scanned area is 2 μm × 2 μm.

could be improved by the use of different solvents and/or a buffer layer. With enhanced V_{OC} and FF values, the performance of the P3S-based polymer solar cells could be improved.

EXPERIMENTAL SECTION

Instrumentation. ^{1}H and ^{13}C NMR spectra were recorded on Bruker AVANCE 400 spectrometer, with tetramethylsilane as an internal reference. The optical absorption spectra were measured by a Shimadzu UV-3100 UV−vis−NIR spectrometer. The number- and weight-average molecular weights of polymers were determined by gel permeation chromatography (GPC) on Viscotek T60A instrument, using chloroform as eluent and polystyrene as standard. The differential scanning calorimetry (DSC) and thermal gravimetric analysis were made using TA Q100 instrument and operated under a nitrogen atmosphere. Cyclic voltammetry was performed on an AUTOLAB/PG-STAT12 model system with a three-electrode cell in a solution of Bu_4NBF_4 (0.10 M) in acetonitrile at a scan rate of 50 mV/s. Polymer film coatings on ITO anode electrode were formed by the spin-coating method. Atomic force microscopy (AFM) was measured by tapping-mode using Multimode IIIa, Digital Instruments. Electrical characteristics of the TFTs were measured in ambient conditions using both Keithley 2400 and 236 source/measure units. For all measurements, we used channel lengths (L) of 12 μm and channel widths (W) of 120 μm. Field effect mobility was extracted in the saturation regime from the slope of the source-drain current.

Materials. 2,5-Bis(trimethylstannyl)thiophene (**7**),[19] 2,5-bis-(trimethylstannyl)selenophene (**8**),[20] 2,3-bis(4-(3,7-dimetyloctyloxy)-phenyl)-5,8-bis(5′-bromodithien-2-ly)quinoxaline (**13**),[30] and 3,6-bis-(5-bromothiophene-2-yl)-2,5-bis(2-ethylhexyl)pyrrolo[3,4-*c*]pyrrole-1,4(2*H*,5*H*)-dione (**14**)[31] were synthesized according to previously published procedures.

3-(3′,7′-Dimethyoctyl)thiophene (1). A 1.0 M solution 3,7-dimethyloctylmagnesium bromide (50 mL, 0.05 mol) was added dropwise to a solution of 3-bromothiophene (6.24 g, 0.04 mol) and Ni(dppp)Cl_2 (0.67 g, 1.2 mmol) in THF (60 mL) at −20 °C with stirring. The mixture was stirred at RT for 4 h and then poured into water (100 mL) and extracted with ethyl acetate. After drying over anhydrous $MgSO_4$, the solvent was evaporated and the residue was purified by column chromatography on silica gel with hexane as eluent. After drying, the product was obtained as colorless oil. Yield: 6.3 g (70%). Fab-MS: m/z = 225. ^{1}H NMR (300 MHz, $CDCl_3$, δ): 7.22 (d, 1H), 6.92 (s, 1H), 6.90 (d, 1H), 2.61 (m. 2H), 1.1−1.50 (m. 10H), 0.91 (d, 3H), 0.87 (d, 6H). ^{13}C NMR (80 MHz, $CDCl_3$, δ): 143.64, 128.48, 125.25, 119.83, 39.54, 38.05, 37.36, 32.69, 28.19, 28.19, 24.93, 22.93, 22.84, 19.79. Anal. Calcd for $C_{14}H_{24}Se$: C 74.93, H 10.78, S 41.29. Found: C 74.70, H 10.41, S 14.47.

1-Chloro-5,9-dimethyldecan-2-one (2). A 1.0 M solution 3,7-dimethyloctylmagnesium bromide (100 mL, 0.1 mol) was added dropwise to a solution of chloroacetyl chloride (16 mL, 0.2 mol) in THF (30 mL) at −78 °C with stirring. The mixture was stirred at −78 °C for 6 h and then poured into water (100 mL) and extracted with ethyl acetate. After drying over anhydrous $MgSO_4$, the solvent was evaporated. The product was used without further purification. Yield: 7.5 g (34%).

3-(Chloromethyl)-6,10-dimethylundec-1-yn-3-ol (3). A 0.5 M solution of ethynylmagnesium bromide (100 mL, 0.05 mol) was added dropwise to a solution of compound **2** (7.5 g, 0.035 mol) in THF (150 mL) at −60 °C with stirring. The mixture was stirred at −60 °C for 4 h and then poured into water (150 mL) and extracted with ethyl acetate. After drying over anhydrous $MgSO_4$, the solvent was evaporated and the residue was purified by column chromatography on silica gel with hexane as eluent. After drying, the product was obtained as colorless oil. Yield: 4.0 g (48%). Fab-MS: m/z = 243. ^{1}H NMR (300 MHz, $CDCl_3$, δ): 3.67 (d, 1H), 3.61 (d, 1H), 2.57 (s, 1H),

dx.doi.org/10.1021/ma2020112 | *Macromolecules* 2012, 45, 1303−1312

2.51 (s. 1H), 1.2−1.7 (m. 9H), 1.1 (m, 3H), 0.87 (m, 9H). ^{13}C NMR (80 MHz, $CDCl_3$, δ): 83.89, 73.88, 70.92, 53.18, 39.48, 37.28, 37.13, 36.88, 33.01, 31.23, 28.17, 24.91, 22.91, 19.83. Anal. Calcd for $C_{14}H_{25}ClO$: C 68.69, H 10.29, O 6.54. Found: C 67.76, H 10.14, O 6.9.

3-(3′,7′-Dimethyoctyl)selenophene (4). A solution selenium (2 g, 0.025 mol) and sodium borohydride (1.84 g, 0.048 mol) was dissolved in 40 mL of ethanol at 0 °C and for 1 h. Compound **3** (4 g, 0.016 mol) in 20 mL of ethanol was added to solution, and the resulting mixture was stirred at RT for 30 min. The resulting mixture was added slowly to a solution of KOH (2.73 g, 0.048 mmol) in 20 mL of ethanol−H_2O (20:1 v/v) at RT. The mixture was refluxed for 2 h at 90 °C. The reaction mixture was then poured into water and extracted with ethyl acetate. After drying over anhydrous $MgSO_4$, the solvent was evaporated. The mixture and *p*-toluenesulfonic acid monohydrate (0.1 g, 0.5 mmol) in 100 mL of hexane was refluxed for 1 h. After cooling, the mixture poured into water (100 mL) and extracted with ethyl acetate. The extract was successively washed with water, 5% sodium hydrogen carbonate aqueous solution, and brine. After drying over anhydrous $MgSO_4$, the solvent was evaporated and the residue was purified by column chromatography on silica gel with hexane as eluent. After drying, the product was obtained as yellow oil. Yield: 1.9 g (43%). Fab-MS: m/z = 273. ^{1}H NMR (300 MHz, $CDCl_3$, δ): 7.89 (d, 1H), 7.52 (s, 1H), 7.19 (d, 1H), 2.60 (m. 2H), 1.1−1.50 (m. 10H), 0.91 (d, 3H), 0.87 (d, 6H). ^{13}C NMR (80 MHz, $CDCl_3$, δ): 145.66, 131.66, 129.86, 39.54, 37.85, 37.35, 32.69, 29.70, 28.19, 24.91, 22.93, 22.84, 19.80. Anal. Calcd for $C_{14}H_{24}S$: C 61.98, H 8.92. Found: C 61.87, H 8.90.

2-Bromo-3-(3′,7′-dimethyoctyl)thiophene (5). To a stirred solution of compound **1** (3.1 g, 13.8 mmol) in chloroform−acetic acid (1:1 v/v, 150 mL), *N*-bromosuccinimide (NBS) (2.73 g, 15.3 mmol) was added. The mixture was stirred at 0 °C for 1 h and then poured into water (100 mL) and extracted with ethyl acetate. The extract was successively washed with water, 5% sodium hydrogen carbonate aqueous solution, and brine. After drying over anhydrous $MgSO_4$, the solvent was evaporated and the residue was purified by column chromatography on silica gel with hexane as eluent. After drying, the product was obtained as yellow oil. Yield: 4.00 g (95%). Fab-MS: m/z = 303. ^{1}H NMR (300 MHz, $CDCl_3$, δ): 7.16 (d, 1H), 6.79 (d, 1H), 2.60 (m. 2H), 1.12−1.54 (m. 10H), 0.91 (d, 3H), 0.87 (d, 6H). ^{13}C NMR (80 MHz, $CDCl_3$, δ): 143.64, 128.49, 125.26, 108.88, 39.53, 37.24, 37.11, 32.68, 28.20, 27.28, 24.90, 22.93, 22.85, 19.80. Anal. Calcd for $C_{14}H_{23}BrS$: C 55.44, H 7.64, S 10.50. Found: C 55.41, H 7.70, S 10.50.

2-Bromo-3-(3′,7′-dimethyoctyl)selenophene (6). The compound was synthesized using the same method as for compound **5**; using compound **3** (1.9 g, 7 mmol) in chloroform−acetic acid (1:1 v/v, 50 mL), *N*-bromosuccinimide (NBS) (1.32 g, 7.2 mmol) was added. The mixture was stirred at 0 °C for 1 h and then poured into water (100 mL) and extracted with ethyl acetate. The extract was successively washed with water, 5% sodium hydrogen carbonate aqueous solution, and brine. After drying over anhydrous $MgSO_4$, the solvent was evaporated and the residue was purified by column chromatography on silica gel with hexane as eluent. After drying, the product was obtained as yellow oil. Yield: 2.35 g (96%). Fab-MS: m/z = 351. ^{1}H NMR (300 MHz, $CDCl_3$, δ): 7.86 (d, 1H), 7.05 (d, 1H), 2.60 (m. 2H), 1.2−1.60 (m. 10H), 0.91 (d, 3H), 0.87 (d, 6H). ^{13}C NMR (80 MHz, $CDCl_3$, δ): 144.64, 131.35, 130.28, 111.20, 39.52, 37.22, 36.98, 32.70, 28.55, 28.19, 24.89, 22.94, 22.86, 19.82. Anal. Calcd for $C_{14}H_{23}BrSe$: C 48.02, H 6.62. Found: C 47.96, H 6.62.

3,3″-(3′,7′-Dimethyoctyl)-2,2′:5,2″-terthiophene (9). A solution tris(dibenzylideneacetone)dipalladium (0) (0.15 g, 0.16 mmol), tri-*o*-tolyphosphine (0.087 g, 0.28 mmol), compound **7** (0.98 g, 2.4 mmol), and compound **5** (1.52 g, 5.01 mmol) was dissolved in 40 mL of anhydrous toluene under N_2. The solution was heated at 90 °C for 3 h. The mixture was then poured into water and extracted with ethyl acetate. The extract was the successively washed with water and brine. After drying over anhydrous $MgSO_4$, the solvent was evaporated and the residue was purified by column chromatography on silica gel with hexane as eluent. After drying, the product was obtained as a yellow solid. Yield: 1.0 g (78%). Fab-MS: m/z = 528. ^{1}H NMR (300 MHz, $CDCl_3$, δ): 7.17 (d, 2H), 7.05 (d, 2H), 6.92 (s, 2H), 2.80 (m. 4H), 1.13−1.70 (m. 20H), 0.91 (d, 6H), 0.87 (d, 12H). ^{13}C NMR (80 MHz, $CDCl_3$, δ): 140.08, 136.27, 130.54, 130.23, 126.25, 124.01, 39.53, 38.21, 37.35, 33.07, 28.20, 27.18, 24.96, 22.92, 22.83, 19.84. Anal. Calcd for $C_{32}H_{48}S_3$: C 72.67, H 9.15, S 18.19. Found: C 72.70, H 9.02, S 18.14.

3,3″-(3′,7′-Dimethyoctyl)-2,2′:5,2″-terselenophene (10). The compound was synthesized using the same method as for compound **9**, using tris(dibenzylideneacetone)dipalladium(0) (0.15 g, 0.16 mmol), tri-*o*-tolyphosphine (0.087 g, 0.28 mmol), compound **8** (1.1 g, 2.39 mmol), and compound **6** (1.84 g, 5.26 mmol) was dissolved in 40 mL of anhydrous toluene under N_2. The solution was heated at 90 °C for 3 h. The mixture was then poured into water and extracted with ethyl acetate. The extract was the successively washed with water and brine. After drying over anhydrous $MgSO_4$, the solvent was evaporated and the residue was purified by column chromatography on silica gel with hexane as eluent. After drying, the product was obtained as a yellow solid. Yield: 1.2 g (82%). Fab-MS: m/z = 670. ^{1}H NMR (300 MHz, $CDCl_3$, δ): 7.88 (d, 2H), 7.21 (d, 2H), 7.14(s, 2H), 2.60 (m. 4H), 1.13−1.68 (m. 20H), 0.91 (d, 6H), 0.87 (d, 12H). ^{13}C NMR (80 MHz, $CDCl_3$, δ): 143.65, 141.41, 137.44, 133.75, 128.87, 128.83, 39.53, 38.24, 37.35, 33.15, 28.45, 24.96, 22.94, 22.85, 19.86. Anal. Calcd for $C_{32}H_{48}Se_3$: C 57.40, H 7.23. Found: C 57.35, H 7.23.

5,5″-Bis(trimethylstannyl)-3,3″-di(3′,7′-dimethyoctyl)-2,2′:5,2″-terthiophene (11). To a solution of compound **9** (0.9 g, 1.7 mmol) in THF (15 mL), a 1.6 M solution of *n*-BuLi in hexane (2.23 mL, 3.5 mmol) was added, and the mixture was stirred at −78 °C and for 1 h and then 1.0 M solution of trimethyltin chloride (3.5 mL, 3.5 mmol) was added in one portion. The solution was warmed to room temperature and stirred at room temperature for 1 h. The reaction mixture was then poured into water and extracted with ethyl acetate. After drying over anhydrous $MgSO_4$, the solvent was evaporated. The crude product was washed several times by using acetone/methanol (1/10) mixed solvents. The product was dissolved in small amount of $CHCl_3$ and precipitated in methanol at low temperature (−40 °C). Yield: 0.6 g (40%). Fab-MS: m/z = 854. ^{1}H NMR (300 MHz, $CDCl_3$, δ): 7.04 (s, 2H), 6.99 (s, 2H), 2.76 (t. 4H), 1.18−1.69 (m, 20H), 0.91 (d, 6H), 0.87 (t, 12H), 0.37 (s, 18H). ^{13}C NMR (80 MHz, $CDCl_3$, δ): 141.11, 139.98, 138.55, 136.68, 130.22, 126.29, 39.54, 38.21, 37.36, 33.23, 28.20, 27.19, 24.98, 22.84, 19.87, −8.02. Anal. Calcd for $C_{38}H_{64}S_3Sn_2$: C 53.41, H 7.15, S 11.26. Found: C 53.51, H 7.20, S 11.34.

5,5″-Bis(trimethylstannyl)-3,3″-di(3′,7′-dimethyoctyl)-2,2′:5,2″-terselenophene (12). The compound was synthesized using the same method as for compound **11**; using compound **6** (0.7 g, 1 mmol) in THF (15 mL), a 1.6 M solution of *n*-BuLi in hexane (1.3 mL, 2 mmol) was added, and the mixture was stirred at −78 °C and for 1 h and then 1.0 M solution of trimethyltin chloride (2.1 mL, 2.1 mmol) was added in one portion. The solution was warmed to room temperature and stirred at room temperature for 1 h. The reaction mixture was then poured into water and extracted with ethyl acetate. After drying over anhydrous $MgSO_4$, the solvent was evaporated. The crude product was washed several times by using acetone/methanol (1/10) mixed solvents. The product was dissolved in small amount of $CHCl_3$ and precipitated in methanol at low temperature (−60 °C). Yield: 0.41 g (52%). Fab-MS: m/z = 996. ^{1}H NMR (300 MHz, $CDCl_3$, δ): 7.37 (s, 2H), 6.81 (s, 2H), 2.73 (t. 4H), 1.18−1.69 (m, 20H), 0.91 (d, 6H), 0.87 (t, 12H), 0.36 (s, 18H). ^{13}C NMR (80 MHz, $CDCl_3$, δ): 144.01, 143.76, 143.44, 141.28, 133.73, 128.90, 39.54, 38.24, 37.36, 33.16, 28.38, 28.20, 24.98, 22.86, 19.87, −7.69. Anal. Calcd for $C_{38}H_{64}Se_3Sn_2$: C 45.86, H 6.48. Found: C 45.90, H 6.50.

P3TDTQ. A 100 mL Schlenk flask containing anhydrous chlorobenzene (10 mL), compound **11** (0.17 g, 0.2 mmol), compound **12** (0.18 g, 0.2 mmol), tris(dibenzylideneacetone)dipalladium(0) (0.01 g, 0.01 mmol), and tri(*o*-tolyl)phosphine (6 mg, 0.02 mmol) was kept under a nitrogen atmosphere at 130 °C for 72 h. When the reaction had finished, reaction mixture was precipitated from the 10 mL of HCl and 150 mL of methanol. The polymer was dissolved in

small amount of $CHCl_3$ and precipitated in methanol. The resulting polymer was further purified by Soxhlet extraction using methanol and hexane then dried in vacuum to give dark-green solid. Yield: 0.2 g (77%). ^{1}H NMR (300 MHz, $CDCl_3$, δ): 8.08 (br, 2H) 7.81 (br, 6H) 7.12 (br, 6H) 6.92 (br, 6H), 4.04 (br, 4H), 2.80 (br, 4H) 1.24−0.81 (m, 76H). Anal. Calcd for $C_{79}H_{100}N_2O_2S_5$: C 70.81, H 8.24, N 2.66, O 3.04, S 15.24. Found: C 70.72, H 8.28, N 2.66, O 3.27, S 15.21.

P3SDTQ. The compound was synthesized using the same method as for P3TDTQ, with compound **12** (0.2 g, 0.2 mmol), compound **13** (0.18 g, 0.2 mmol), tris(dibenzylideneacetone)dipalladium(0) (0.01 g, 0.01 mmol), tri(*o*-tolyl)phosphine (6 mg, 0.02 mmol), and chlorobenzene (10 mL) being kept under a nitrogen atmosphere at 130 °C for 72 h. When the reaction had finished, reaction mixture was precipitated from the 10 mL of HCl and 150 mL of methanol. The polymer was dissolved in small amount of $CHCl_3$ and precipitated in methanol. The resulting polymer was further purified by Soxhlet extraction using methanol and hexane then dried in vacuum to give dark-green solid. Yield: 0.17 g (80%). ^{1}H NMR (300 MHz, $CDCl_3$, δ): 8.09 (br, 2H) 7.81(br, 6H) 7.19 (br, 6H) 6.92 (br, 6H), 4.08 (br, 4H), 2.82 (br, 4H) 1.55−0.81 (m, 76H). Anal. Calcd for $C_{79}H_{100}N_2O_2S_2Se_3$: C 67.26, H 7.15, N 1.99, O 2.27, S 4.55. Found: C 67.19, H 7.29, N 1.84, O 2.45, S 4.16.

P3TDTDPP. The compound was synthesized using the same method as for P3TDTQ, with compound **11** (0.17 g, 0.2 mmol), compound **14** (0.136 g, 0.2 mmol), tris(dibenzylideneacetone)-dipalladium(0) (0.01 g, 0.01 mmol), tri(*o*-tolyl)phosphine (6 mg, 0.02 mmol), and chlorobenzene (10 mL) being kept under a nitrogen atmosphere at 130 °C for 72 h. When the reaction had finished, reaction mixture was precipitated from the 10 mL of HCl and 150 mL of methanol. The polymer was dissolved in a small amount of $CHCl_3$ and precipitated in methanol. The resulting polymer was further purified by Soxhlet extraction using methanol and hexane then dried in vacuum to give dark solid. Yield: 0.17 g (62%). ^{1}H NMR (300 MHz, $CDCl_3$, δ): 8.98−8.90 (br, 2H), 7.18−6.92 (br, 6H), 4.03 (br, 4H) 2.77 (br, 4H) 1.92−0.86 (m, 68H). Anal. Calcd for $C_{79}H_{100}N_2O_2S_5$: C 74.72, H 8.15, N 2.18, O 2.49, S 12.47. Found: C 74.35, H 8.04, N 2.44, O 2.37, S 12.84.

P3SDTDPP. The compound was synthesized using the same method as for P3TDTQ, with compound **12** (0.2 g, 0.2 mmol), compound **14** (0.136 g, 0.2 mmol), tris(dibenzylideneacetone)-dipalladium(0) (0.01 g, 0.01 mmol), tri(*o*-tolyl)phosphine (6 mg, 0.02 mmol), and chlorobenzene (10 mL) being kept under a nitrogen atmosphere at 130 °C for 72 h. When the reaction had finished, reaction mixture was precipitated from the 10 mL of HCl and 150 mL of methanol. The polymer was dissolved in small amount of $CHCl_3$ and precipitated in methanol. The resulting polymer was further purified by Soxhlet extraction using methanol and hexane and then dried in a vacuum to give a dark solid. Yield: 0.13 g (54%). ^{1}H NMR (300 MHz, $CDCl_3$, δ): 8.96−8.89 (br, 2H), 7.82−6.82 (br, 6H), 4.02 (br, 4H) 2.69 (br, 4H) 1.91−0.87 (m, 68H). Anal. Calcd for $C_{62}H_{86}N_2O_2S_2Se_3$: C 62.45, H 7.25, N 2.35, O 2.68, S 5.38. Found: C 62.26, H 7.28, N 2.21, O 2.91, S 5.18.

Fabrication of the Organic Thin Film Transistors (OTFTs). OTFT devices were fabricated in a bottom-contact geometry (channel length = 12 μm, width = 120 μm). The source and drain contacts consisted of gold (100 nm), and the dielectric was silicon oxide (SiO_2) with a thickness of 300 nm. The SiO_2 surface was cleaned, dried, and pretreated with a solution of 1.0 mM octyltrichlorosilane (OTS-8) in toluene at room temperature for 2 h under nitrogen to produce nonpolar and smooth surfaces onto which the polymers could be spin-coated. The polymers were dissolved to a concentration of 0.5 wt % in chlorobenzene. Films of the organic semiconductors were spin-coated at 1500 rpm for 50 s to a thickness of 50 nm, followed by an annealing process. All device fabrication procedures and measurements were carried out in air at room temperature.

Fabrication of the Polymer Solar Cells (PSCs). In this study, the devices were fabricated with the structure ITO/PEDOT:PSS/polymer:$PC_{61}BM$ or $PC_{71}BM$/LiF/Al. The procedure for cleaning the ITO surface included sonication and rinsing in deionized water, methanol, and acetone. The hole-transporting PEDOT:PSS layer was spin-coated onto each ITO anode from a solution purchased from H.C. Starck and baked for 20 min at 140 °C in a glovebox. Each polymer:$PC_{61}BM$ solution was then spin-coated onto the PEDOT:PSS layer. The polymer solution for spin-coating was prepared by dissolving the polymer (1 wt %) in chlorobenzene. Preannealing was not carried out. LiF and aluminum contacts were formed by vacuum deposition at pressures below 3×10^{-6} Torr, providing an active area of 0.09 cm^2. Solar cell efficiencies were characterized under simulated 100 mW/cm^2 AM 1.5G irradiation from a Xe arc lamp with an AM 1.5 global filter. Simulator irradiance was characterized using a calibrated spectrometer, and the illumination intensity was set using an NREL certified silicon diode with an integrated KG1 optical filter. The EQE was measured by underfilling the device are a using a reflective microscope objective to focus the light output from a 100 W halogen lamp outfitted with a monochromator and optical chopper; the photocurrent was measured using a lock-in amplifier, and the absolute photon flux was determined using a calibrated silicon photodiode. All device fabrication procedures and measurements were carried out in air at room temperature.

■ ASSOCIATED CONTENT

Ⓢ Supporting Information

IV characteristics and AFM images of the polymers. This material is available free of charge via the Internet at http://pubs.acs.org.

■ AUTHOR INFORMATION

Corresponding Author

*E-mail: inamkang@catholic.ac.kr.

■ ACKNOWLEDGMENTS

This research was supported by Basic Science Research Program through the National Research Foundation of Korea (NRF) funded by the Ministry of Education, Science and Technology (2011-0004016), also supported by the New & Renewable Energy of the Korea Institute of Energy Technology Evaluation and Planning (KETEP) grant funded by the Korea government Ministry of Knowledge Economy (2011T100200034), and by a grant from the cooperative R&D Program (B551179-08-03-00) funded by the Korea Research Council Industrial Science and Technology, Republic of Korea

■ REFERENCES

(1) Chen, H.-Y.; Hou, J. H.; Zhang, S. Q.; Liang, Y.; Yang, G. W.; Yang, Y.; Yu, L. P.; Wu, Y.; Li, G. *Nature Photonics* **2009**, *3*, 649.

(2) Yu, G.; Gao, J.; Hummelen, J. C.; Wudl, F.; Heeger, A. J. *Science* **1995**, *270*, 1789.

(3) Koetse, M. M.; Sweelssen, J.; Hoekerd, K. T.; Schoo, H. F. M.; Veenstra, S. C.; Kroon, J. M.; Yang, X.; Loos.. *J. Appl. Phys. Lett.* **2006**, *88*, 83504.

(4) Wienk, M. M.; Koon, J. M.; Verhees, W. J. H.; Knol, J.; Hummelen, J. C.; van Hal, P. L.; Janssen, R. A. J. *Angew. Chem., Int. Ed.* **2003**, *42*, 3371.

(5) Lee, S. K.; Cho, J. K.; Goo, Y.; Shin, W. S.; Lee, J.-C.; Lee, W.-H.; Kang, I.-N.; Shim, H.-K.; Moon, S.-J. *Chem. Commun.* **2011**, *47*, 1791−1793.

(6) Guänes, S.; Neugebauer, H.; Sariciftci, N. S. *Chem. Rev.* **2007**, *107*, 1324.

(7) Thompson, B. C.; Frechet, J. M. J. *Angew. Chem., Int. Ed.* **2008**, *47*, 58.

(8) Peet, J.; Kim, J. Y.; Coates, N. E.; Ma, W. L.; Moses, D.; Heeger, A. J.; Bazan, G. C. *Nature Mater.* **2007**, *6*, 497−500.

(9) Chen, H.-Y.; Hou, J.; Hayden, A. E.; Yang, H.; Houk, K. N.; Yang, Y. *Adv. Mater.* **2010**, *22*, 371−375.

(10) Kim, B.; Yeo, J. S.; Khim, D.; Kim, D.-Y. *Macromol. Rapid Commun.* **2011**, DOI: 10.1002/marc.201100327.
(11) Zou, Y.; Gendron, D.; Neagu, R.; Leclerc, M. *Macromolecules* **2009**, *42*, 6361.
(12) Wang, E.; Hou, L.; Wang, Z.; Hellström, S.; Zhang, F.; Inganäs, O.; Andersson, M. R. *Adv. Mater.* **2010**, *22*, 5240.
(13) Zade, S. S.; Zamoshchik, N.; Bendikov, M. *Chem.—Eur. J.* **2009**, *15*, 8613.
(14) Ballantyne, A. M.; Chen, L. C.; Nelson, J.; Bradley, D. D. C.; Astuti, Y.; Maurano, A.; Shuttle, C. G.; Durrant, J. R.; Heeney, M.; Duffy, W.; McCulloch, I. *Adv. Mater.* **2007**, *19*, 4544.
(15) Heeney, M.; Zhang, W.; Crouch, D. J.; Chabinyc, M. L.; Gordeyev, S.; Hamilton, R.; Higgins, S. J.; McCulloch, I.; Skabara, P. J.; Sparrowe, D.; Tierney, S. *Chem. Commun.* **2007**, *43*, 5061.
(16) Chen, Z. Y.; Lemke, H.; Albert-Seifried, S.; Caironi, M.; Nielsen, M. M.; Heeney, M.; Zhang, W. M.; McCulloch, I.; Sirringhaus, H. *Adv. Mater.* **2010**, *22*, 2371.
(17) Crouch, D. J.; Skabara, P. J.; Heeney, M.; McCulloch, I.; Sparrowe, D.; Coles, S. J.; Hursthouse, M. B. *Macromol. Rapid Commun.* **2008**, *29*, 1839−1843.
(18) Ha, J. S.; Kim, K. H.; Choi, D. H. *J. Am. Chem. Soc.* **2011**, DOI: 10.1021/ja203189h.
(19) Furuta, P.; Fréchet, J. M. J. *J. Am. Chem. Soc.* **2003**, *125*, 13173−13181.
(20) Martin, H.; Warren, D.; Iain, M.; Simon, H.; David, C.; Peter, S. EP2006/010421.
(21) Koppe, M.; Scharber, M.; Brabec, C.; Duffy, W.; Heeney, M.; McCulloch, I. *Adv. Funct. Mater.* **2007**, *17*, 1371.
(22) Patra, A.; Wijsboom, Y. H.; Zade, S. S.; Li, M.; Sheynin, Y.; Leitus, G.; Bendikov, M. *J. Am. Chem. Soc.* **2008**, *130*, 6734.
(23) Salzner, U.; Lagowski, J. B.; Pickup, P. G.; Poirier, R. A. *Synth. Met.* **1998**, *96*, 177.
(24) Cheng, Y.-J.; Wu, J.-S.; Shih, P.-I.; Chang, C.-Y.; Jwo, P.-C.; Kao, W.-S.; Hsu, C.-S. *Chem. Mater.* **2011**, *23*, 2361.
(25) Bijleveld, J. C.; Zoombelt, A. P.; Mathijssen, S. G. J.; Wienk, M. M.; Turbiez, M.; de Leeuw, D. M.; Janssen, R.A. J. *J. Am. Chem. Soc.* **2009**, *131*, 16616.
(26) Huo, L.; Hou, J.; Chen, H.-Y.; Zhang, S.; Jiang, Y.; Chen, T. L.; Yang, Y. *Macromolecules* **2009**, *42*, 6564.
(27) Rusling, J. F.; Suib, S. L. *Adv. Mater.* **1994**, *6*, 922.
(28) Dimitrakoupoulos, C. D.; Melenfant, R. M. *Adv. Mater.* **2002**, *14*, 99.
(29) Halls, J. J. M.; Pichler, K.; Friend, R. H.; Moratti, S. C.; Holmes, A. B. *Appl. Phys. Lett.* **1996**, *68*, 3120.
(30) Lee, S. K.; Lee, W.-H.; Cho, J. M.; Park, S. J.; Shin, W. S.; Lee, J.-C.; Kang, I.-N.; Moon, S.-J. *Macromolecules* **2011**, *44*, 5994−6001.
(31) Huo, L.; Hou, J.; Chen, H.-Y.; Zhang, S.; Jiang, Y.; Chen, T. L.; Yang, Y. *Macromolecules* **2009**, *42*, 6564.